Applied Thermal Engineering 31 (2011) 820–826

Contents lists available at ScienceDirect

Applied Thermal Engineering

journal homepage: www.elsevier.com/locate/apthermeng

Heat transfer correlations of forced convective boiling for pure refrigerants in micro-fin tubes

C.B. Chiou [a,*], D.C. Lu [b], C.C. Chen [a], C.M. Chu [c]

[a] Department of Automatic & Control Engineering, ChungChou Institute of Technology, Yuanlin ChangHua 510, Taiwan
[b] Department of Mechanical Engineering, National Chiao Tung University, Hsinchu 300, Taiwan
[c] Graduate School of Engineering Technology, ChungChou Institute of Technology, Yuanlin ChangHua 510, Taiwan

ARTICLE INFO

Article history:
Received 26 December 2009
Accepted 29 October 2010
Available online 18 November 2010

Keywords:
Forced convective boiling
Evaporation
Pure refrigerant
Micro-fin
Correlation

ABSTRACT

The evaporation heat transfer coefficient of pure refrigerants R-22 and R-124 in micro-fin tubes were measured at the reduced pressure of 0.15, the mass flux from 100 to 400 kg/m^2 s, the flow quality from 0.1 to 0.9, and the heat flux from 5 to 20 kW/m^2. The evaporation heat transfer coefficient of pure refrigerant in micro-fin tube is 1.5–3.0 times higher than that of smooth tube. In this article, the single phase forced convection heat transfer coefficient of micro-fin tube is introduced to predict the evaporation heat transfer coefficient of pure refrigerant in micro-fin tubes. The present correlations provide reasonable agreement with the experimental data. The prediction values mostly fall within ±30%.

1. Introduction

Micro-fin tubes are usually used in air conditioners and refrigerators to improve the thermal performance of finned tube heat exchangers. Many experimental studies of boiling heat transfer have been investigated inside horizontal micro-fin tubes. Yoshida et al. [1] have measured the heat transfer coefficient of R-22 in micro-fin tube, the result at mass flux $G = 300$ kg/m^2 s shows that the heat transfer enhancement amount of micro-fin tube is about 1.5 times that of smooth tube. Khanpara et al. [2] have measured the evaporation heat transfer coefficient of R-113 in micro-fin tube, the result shows that the heat transfer coefficient is enhanced by 30–100% than that of smooth tube and the pressure drop is increased by about 80%. Sohlagger et al. [3], Eckels et al. [4], Kim and Shin [5], Chiang [6], and Greco et al. [7] have shown that the heat transfer coefficient of micro-fin tube is higher than that of smooth tube, and the average heat transfer enhancement amount is about 1.6–3.2 times. Thome [8] has summarized the causes for the enhancement of the heat transfer coefficient of micro-fin tube as in the followings:

1. The overall heat transfer area is increased.
2. At low flow rate, the rinsing area at the direction of circumference is larger.
3. There are more nucleate cavity sites.
4. There is flow field turbulence caused by the fins.

During the past decades, many aspects of boiling heat transfer have been investigated in micro-fin tubes. However, the generalized correlation for evaporation heat transfer in micro-fin tubes is a lack in the literatures. The main objective of this article is to develop the heat transfer correlations of pure refrigerants inside horizontal micro-fin tubes.

2. Experimental system

Fig. 1 illustrates the experimental system. It can be observed that the entire experimental system can be divided into four sections, i.e., a condensing system, refrigerant circulation system, pre-heater system, and hot water system.

2.1. Condensing system

The condensing system consists of a thermostat that provides chilled water, a condenser, and a subcooler. After the refrigerant vapor exits the test section, it enters the condenser, and the chilled water provided by the thermostat condenses the refrigerant vapor into a saturated liquid. Before the refrigerant enters the refrigerant flow meter, it passes through the subcooler so as to ensure that the refrigerant entering the flow meter is in a liquid state and to facilitate the refrigerant flow rate measurement. In addition, the flow rate and

* Corresponding author. Tel.: +886 4 8311498x2545; fax: +886 4 8394076.
E-mail address: ccbiau@so-net.net.tw (C.B. Chiou).

1359-4311/$ – see front matter © 2010 Elsevier Ltd. All rights reserved.
doi:10.1016/j.applthermaleng.2010.10.031

Nomenclature

A	heat transfer area, m^2
AE	average error
Cp	specific heat, J kg^{-1} K^{-1}
d	tube diameter, m
e	fin height, m
$e+$	roughness Reynolds number
f	friction factor
G	mass flux, kg m^{-2} s^{-1}
$\bar{g}(e^+)$	correlation parameter
h	heat transfer coefficient, W m^{-2} K^{-1}
h_{tp}	two phase heat transfer coefficient, W m^{-2} K^{-1}
i_{fg}	latent heat, J kg^{-1}
k	thermal conductivity, W m^{-1} K^{-1}
LMTD	logarithm mean temperature difference, K
M	molecular weight, g mol^{-1}
m	mass flow rate, kg s^{-1}
m_r	refrigerant mass flow rate, kg s^{-1}
N_p	numbers of experimental data
Nu	Nusselt number, $h_l\, d_i\, k^{-1}$
n_f	fin number
p_c	critical pressure
Pr	Prandtl number, $\mu\, C_p\, k^{-1}$
p	fin pitch, m
p_r	reduced pressure, P Pc^{-1}
S	average heat transfer rate, W
q'	heat flux, W m^{-2}
Re	Reynolds number, $G\, d_i \mu^{-1}$
R_w	wall resistance, K W^{-1}
r_{cr}	critical radius, m
SD	Standard deviation
St	Stanton number, Nu Re^{-1} Pr^{-1}
T	temperature, K
T_b	bubble point temperature, K
T_d	dew point temperature, K
ΔT	temperature difference, K
ΔT_{ab}	temperature difference between dew point and bubble point, K
ΔT_{id}	ideal temperature difference, K
ΔT_0	reference temperature difference, K
U	overall heat transfer coefficient, W m^{-2} K^{-1}
X_f	flow quality
Xb, Xg, Xr	correlation parameter
X_{tt}	Martinelli parameter
x	mass concentration of volatile component
Yb,Yg	correlation parameter

Greek letters

α	helix angle
δ_w	wall thickness, m
ν	kinematic viscosity, m^{-2} s^{-1}
μ	dynamic viscosity, kg m^{-1} s^{-1}
ρ	density, kg m^{-3}
σ	surface tension, N m^{-1}

Subscripts

b	bubble point
cal	calculation
d	dew point
exp	experiment
i	inside
id	ideal
in	inlet
l	liquid
lo	liquid only
o	outside
p	pure refrigerant
p1	pure refrigerant 1
p2	pure refrigerant 2
tp	two phase
v	vapor

temperature of the chilled water entering the condenser can be adjusted so as to maintain a stable system pressure.

2.2. Refrigerant circulation system

The main components of the refrigerant circulation system include a refrigerant pump, needle valve, dryer and filter, refrigerant flow meter, and test section. The refrigerant pump is a gear pump with an input voltage of 220 V and an output power of 373 W. The refrigerant pump is connected to an inverter that can be used to adjust the rotational speed of the pump and the refrigerant flow rate.

The test section consists of a double tube with hot water flowing on the shell side and the refrigerant on the tube side. Thus, a counter flow is produced between the shell and tube sides. Pressure gauges are installed at both the entrance and exit ends of the test section to measure the pressure in the system. The exterior of the test section is coated with an insulation material of 50 mm thickness to prevent heat losses. The experiment is carried out with four stages of test section. The test tube was divided into four sections with the length of each section as 1.2 m. The advantage of using four stages experiment is that the adjustment of primary inlet quality can measure simultaneously four sets of heat transfer coefficients under different qualities. Therefore, the time needed for the experiment can be greatly reduced. The entrance and exit ends of each sub-section are installed with T-type thermocouples so as to measure the temperature of the water and refrigerant. The overall length of the test tube is 4.8 m, the outer diameter is 9.52 mm, and inner diameter is 8.96 mm. The shell tube in the test section is a copper tube that has an outer diameter of 15.875 mm and an inner diameter of 13.875 mm. Furthermore, a sight glass tube is used to be connected the test tube at each small section. The flow pattern of the refrigerant mixture can be observed through the sight glass.

2.3. Pre-heater system

Pre-heater is a double tube heat exchanger with its shell side filled with hot water, and the flow rate and temperature of the hot water are controlled to control the flow quality of the refrigerant exiting the pre-heater.

2.4. Hot water system

Hot water system includes a hot water tank that has a heating capability of 5 kW and a hot water pump of 373 W. The hot water pump is connected to an inverter so as to adjust the flow rate of the hot water at the test section.

Table 1 is the geometrical parameters of the test tubes. Table 2 presents the test conditions of the experiment. The mass flux ranged from 100 to 400 kg/m^2 s; flow quality ranged between 0.1 and 0.9; and the heat flux varied between 5, 10, and 20 kW/m^2. The

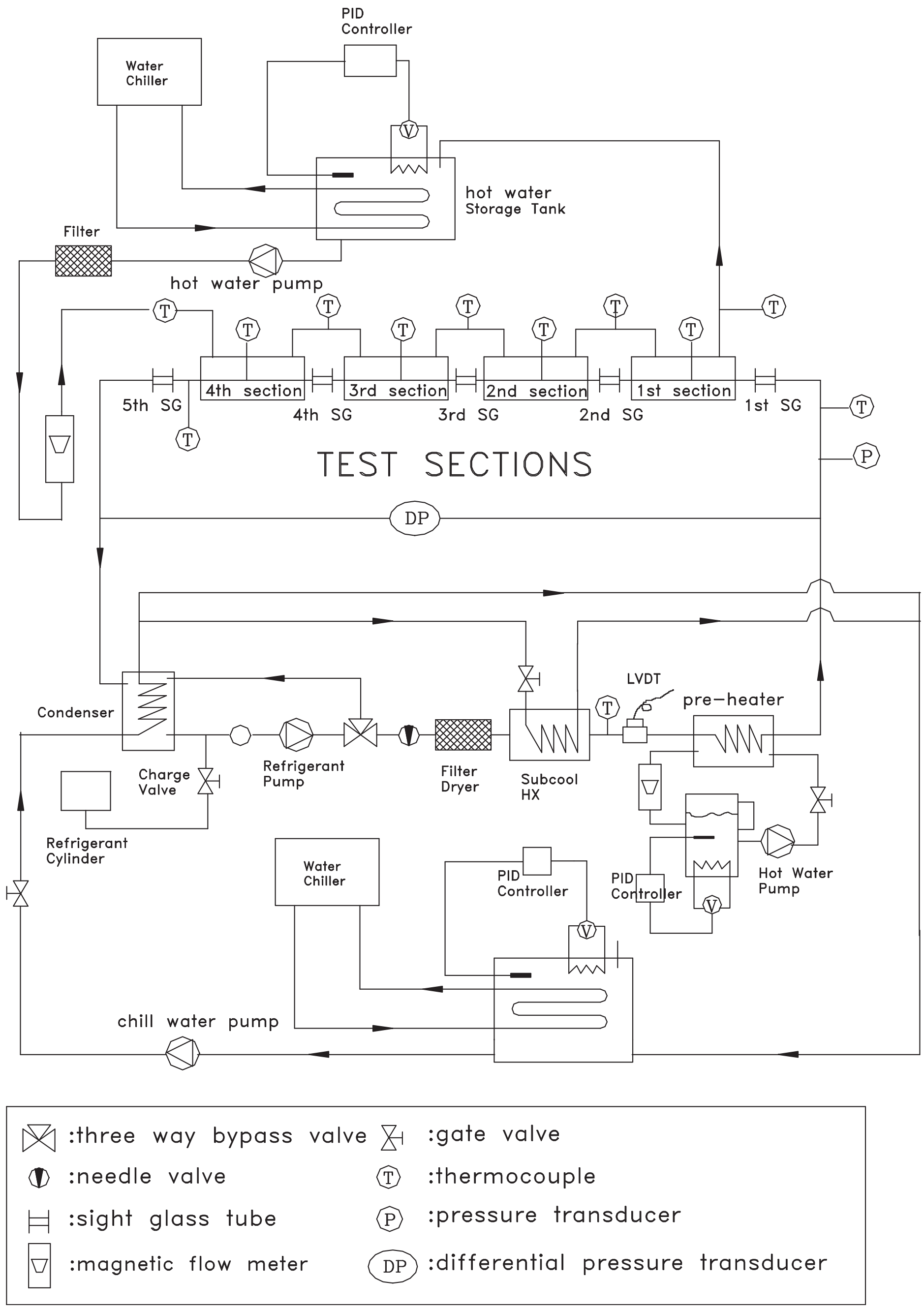

Fig. 1. Schematic diagram of test apparatus.

pressure is represented by a reduced pressure which is defined as the ratio between saturated pressure and critical pressure. During the experimental process, we have adjusted the flow rate and temperature of chill water of condenser so as to change the saturated pressure of the system and to let reduced pressure maintain at constant value of 0.15.

Since the T-type thermocouple used in this system has been calibrated by a HP2804A-type quartz thermometer, the error in the measurement accuracy can be as small as ± 0.1 °C. The error in the measurement accuracy of the refrigerant and hot water flow meter after calibration can reach ± 0.001 l/s and that of the pressure gauge can reach $\pm 0.02\%$. All the measurement signals, for example, temperature and voltage, pass through a personal computer HP3852 and get recorded therein. Table 3 presents the experimental uncertainty calculated by the method suggested by Moffat [9]. It can be observed that the uncertainty of the heat transfer coefficient within the tube is 8%.

Table 4 provides the measurement values of the heat loss at the test section. The measurement of heat loss was performed before loading the refrigerant into the system. After the tube side was evacuated, the shell side of the test section was filled with hot water, and the temperature difference between the entrance and the exit of the hot water was measured so as to calculate the heat lost to the environment on the hot water side of the test section. During the experiment, the variation in the hot water flow rate at the shell side was 1–5 kg/min, and it can be observed from Table 4 that the heat loss of this system was very small, i.e., even when the hot water flow rate was 1 kg/min, the heat loss was merely 21.4 W.

Table 5 presents the error in the energy measurement between the refrigerant side and the hot water side at the test section.

Table 1
Geometrical parameters of test tubes.

	d_0 (mm)	d_i (mm)	δ_w (mm)	e (mm)	α (°)	n_f
Tube #1	9.52	8.96	0.36	0.20	18	60
Tube #2	9.52	8.96	0.41	0.15	25	65

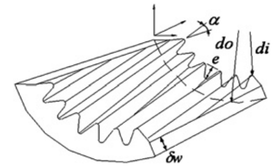

During the test, the subcooled liquid refrigerant enters the test section, and then the hot water is used to heat the refrigerant into a superheated vapor. By calculating the enthalpy difference between the entrance and exit of the refrigerant, the heat transfer at the refrigerant side can be calculated. It can be observed from the Table 5 that at $G = 100$ kg/m^2 s, the heat capacity error is 6%, and when $G = 300$ kg/m^2 s, the heat capacity error is 2%. Therefore, the temperature and flow rate measurements performed in this system at both the refrigerant side and hot water side are highly accurate.

3. Data analysis

If the temperature of the subcooled liquid refrigerant entering the pre-heater is T_l, refrigerant flow rate is m_r, the heat transfer provided by the hot water of the pre-heater is Q_{pre} wherein Q_{pre} includes the sensible heat required to heat the refrigerant from the subcooled liquid to the saturated state and the latent heat required to heat the refrigerant in the saturated state to attain a inlet quality $X_{f,in}$, the quality at the entrance of the test section can be calculated as follows:

$$X_{f,in} = \frac{1}{i_{fg}}\left[\frac{Q_{pre}}{m_r} - Cp_l(T_{b,in} - T_l)\right] \tag{1}$$

If the amount of heat transferred at the first section of the test tube is Q_1, then the quality at the exit of the first section is

$$X_{f,1} = X_{f,in} + \frac{Q_1}{m_r i_{fg}} \tag{2}$$

However, the flow quality in the first section is defined as

$$X_{f,1ave} = \frac{X_{f,in} + X_{f,1}}{2} \tag{3}$$

Similarly, we can obtain the flow quality at the exit and the average flow quality in the other sections.

The relationship between the overall heat resistance and the individual heat resistances in the test section can be expressed as

$$\frac{1}{U_o A_o} = \frac{1}{h_o A_o} + R_w + \frac{1}{h_{tp} A_i} \tag{4}$$

wherein $R_w = \delta_w/(k_w A_w)$ is the thermal resistance at the tube wall,

$$U_o = \frac{Q_{water}}{\mathrm{LMTD} \times A_o} \tag{5}$$

$$Q_{water} = (mCp\Delta T)_{water} \tag{6}$$

$$\mathrm{LMTD} = \frac{\Delta T_1 - \Delta T_2}{\ln\left(\frac{\Delta T_1}{\Delta T_2}\right)} \tag{7}$$

$$\Delta T_1 = T_{water,in} - T_{b,out} \tag{8}$$

$$\Delta T_2 = T_{water,out} - T_{b,in} \tag{9}$$

$T_{b,in}$ and $T_{b,out}$ are the bubble point temperatures of the refrigerant at the entrance and the exit of the test section, respectively, calculated by using the REFPROP [10] program. The heat transfer coefficient of hot water h_0 at the shell side is 1966 W m^{-2} K^{-1}, which can be obtained by means of Wilson plot techniques [11]. Equation (4) can be used to calculate the experimental evaporation heat transfer coefficient h_{tp} for the refrigerants.

4. Results and discussions

Figs. 2 and 3 are diagrams showing respectively the change of the ratio of two phase heat transfer coefficient to single phase heat transfer coefficient versus $1/X_{tt}$ for refrigerants R-22 and R-124, wherein h_{tp} is the evaporation heat transfer coefficient, X_{tt} is Martinelli parameter and $h_{lo,f}$ is the single phase forced convection heat transfer coefficient for micro-fin tube, which can be acquired from our past research [12], and the related parameters are defined as in the followings:

$$h_{lo,f} = G \cdot Cp_l \cdot St \tag{10}$$

$$St = \frac{\frac{f}{2}}{1 + \sqrt{\frac{f}{2}}\left[\bar{g}(e^+)\mathrm{Pr}_l^{0.59} - B(e^+)\right]}, \quad \text{for } 2500 \le \mathrm{Re}_l \le 40000 \tag{11}$$

$$\mathrm{Re}_l = \frac{G d_i}{\mu_l} \tag{12}$$

Table 2
Test conditions.

parameters	Range
Reduced pressure (p_r)	0.15
Quality (X_f)	0.1–0.9
Mass flux (G, kg/m^2 s)	100, 200, 300, 400
Heat flux (q', kW/m^2)	5, 10, 20

Table 3
Uncertainties of test parameters.

Primary uncertainties		Derived uncertainties %	
T	0.1 °C	ΔT	2
d_i	0.01 mm	A_i	1
l	2 mm	Q	4
m_r	0.001 kg/s	U	5
m_{water}	0.001 kg/s	h_{tp}	8

Table 4
Heat loss at test section.

Hot water mass flow rate	1 kg/min	5 kg/min
Heat loss	21.4 W	8.2 W

Table 5
Energy error of refrigerant side and hot water side.

G (kg/m^2 s)	Q_{ref} (W)	Q_{water} (W)	$Q_{ave} = \frac{Q_{ref}+Q_{water}}{2}$ (W)	$\frac{\lvert Q_{ave}-Q_{water}\rvert}{Q_{ave}}$%
100	1136.8	1282.9	1209.9	6
200	2239.7	2375.4	2307.6	3
300	3372.7	3465.9	3419.3	2

$$f = 2\left(e^{+}/[(e/d_{i})\mathrm{Re}_{l}]\right)^{2} \tag{13}$$

$$e^{+} = 0.1407 + 0.093675X_{r} + 0.58464/\ln(X_{r}) \quad \text{for } e^{+} \le 23 \tag{14}$$

$$e^{+} = 0.07313 + 0.09571X_{r} \quad \text{for } e^{+} > 23 \tag{15}$$

$$X_{r} = \mathrm{Re}_{l}\left(\frac{e}{d_{i}+0.005}\right)\frac{n_{f}^{0.25}}{(\cos\alpha)^{0.5}} \tag{16}$$

$$B\left(e^{+}\right) = [\exp(Y_{b})]X_{b} \tag{17}$$

$$Y_{b} = 2.45805 - 0.98726\ln e^{+} \tag{18}$$

$$X_{b} = \mathrm{Re}_{l}\left(\frac{e}{d_{i}}\right)\left(\frac{\cos\alpha}{n_{f}^{0.7}}\right) \tag{19}$$

$$\bar{g}\left(e^{+}\right) = Y_{g}X_{g} \tag{20}$$

$$X_{g} = \frac{n_{f}(\tan\alpha)^{0.1}}{\left(\frac{e}{d_{i}}\right)^{0.4}} \tag{21}$$

$$Y_{g} = 0.007705 + 0.321\left(\ln e^{+}\right)/e^{+} \quad \text{for} \quad e^{+} \le 23 \tag{22}$$

$$Y_{g} = 0.06501 - 0.51903/e^{+} + 5.5956/\left(e^{+}\right)^{2} \quad \text{for} \quad e^{+} > 23 \tag{23}$$

It can be seen from Fig. 2 that heat flux has a notable effect on the evaporation heat transfer coefficient. Therefore, when the heat transfer correlation is constructed, the heat flux effect should be considered. We can use regression analysis to find the correlations among the evaporation heat transfer coefficient, $1/X_{tt}$, heat flux q'', geometrical dimensions of micro-fin tube and refrigerant properties, etc., for pure refrigerant in micro-fin tube, the result is as shown in equation (24):

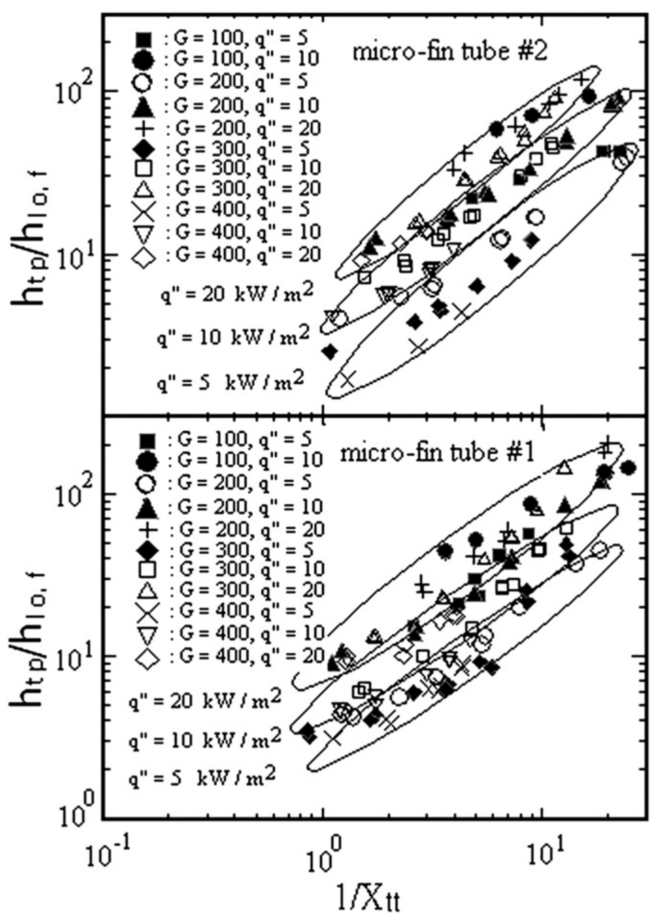

Fig. 2. Relationship between heat transfer coefficient and $1/X_{tt}$ for R-22 at mass flux G = 100–400 kg/m^2 s and heat flux q'' = 5–20 kW/m^2.

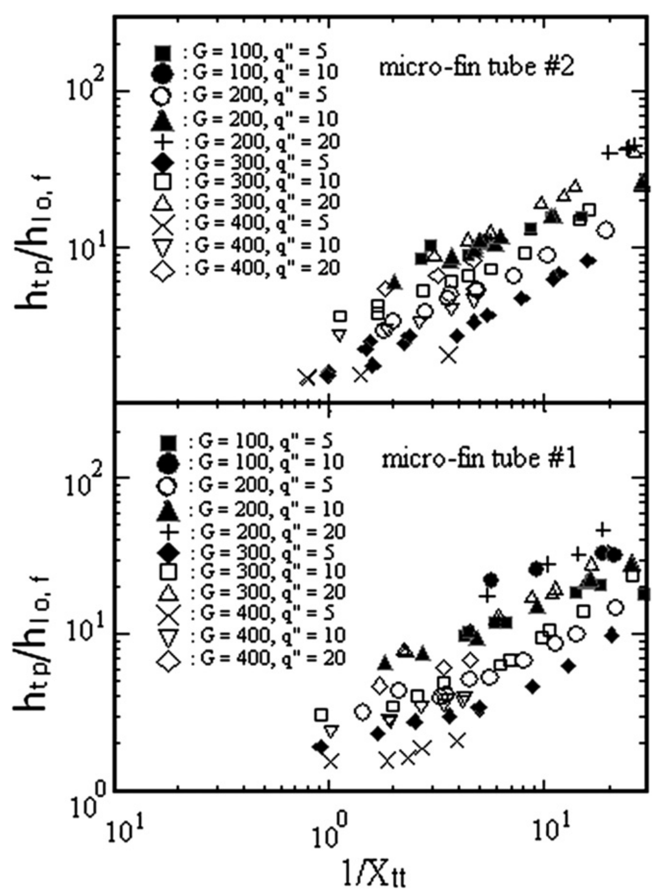

Fig. 3. Relationship between heat transfer coefficient and $1/X_{tt}$ for R-124 at mass flux G = 100–400 kg/m^2 s and heat flux q'' = 5–20 kW/m^2.

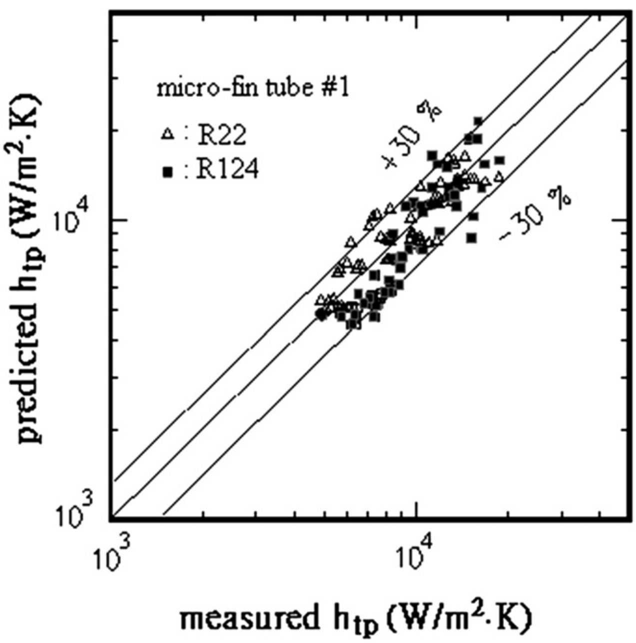

Fig. 4. Comparison of experimental data with predicted heat transfer coefficient for micro-fin tube #1.

$$\ln\left(\frac{h_{tp}}{h_{lo,f}}\right) = -5.75 + (1.01)\ln\left[\left(\frac{1}{X_{tt}}\right)\left(\frac{q''}{q''_{ONB}}\right)^{0.6}\left(\frac{p}{e}\right)(M)\right] \quad (24)$$

wherein M is the molecular weight of refrigerant, e is the fin height, $p = \pi d_i/(n_f \tan\alpha)$ is the fin pitch, the local quality is used to calculate X_{tt} , q''_{ONB} is the heat flux of onset of flow nucleate boiling, Steiner and Taborek [13] recommended that Eqs. (25) and (26) are used to calculate q''_{ONB}.

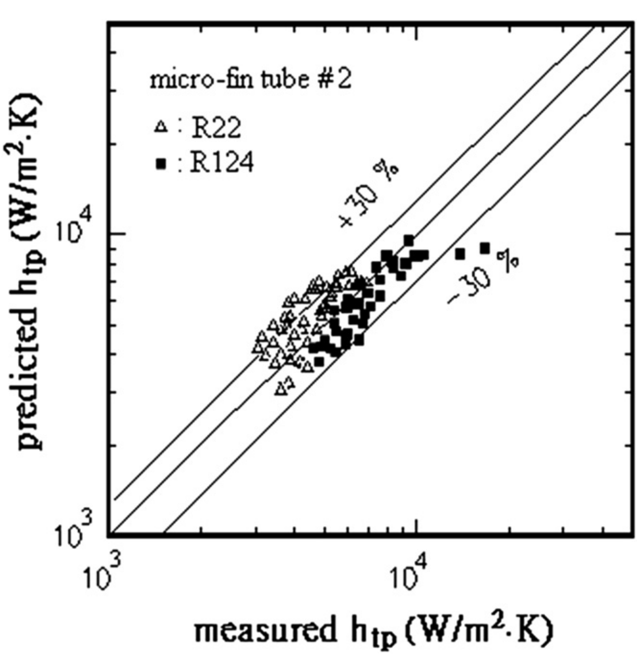

Fig. 5. Comparison of experimental data with predicted heat transfer coefficient for micro-fin tube #2

Table 6
Comparison of average errors and standard deviation for tube #1 and tube #2

Correlations	Tube #1		Tube #2	
	AE %	SD %	AE %	SD %
Eq. (24)	6	25	−1	20

Note: $AE \equiv \frac{\sum[(h_{cal} - h_{exp})/h_{exp}]}{N_p}$, $SD \equiv \sqrt{\frac{\sum[(h_{cal}-h_{exp})/h_{exp}]^2}{N_p}}$

$$q''_{ONB} = \frac{2\sigma T_{sat} h_l}{r_{cr}\rho_v i_{fg}}, \quad r_{cr} = 0.3 \times 10^{-6} \quad (25)$$

$$h_l = 0.023\frac{k_l}{d_i}Re_l^{0.8}Pr_l^{0.4} \quad (26)$$

By the sight glass on the experimental system to view the flow pattern, it can be found that when the mass flux $G \leq 100$ kg/m^2 s, no matter how large the quality of the refrigerant is, its flow pattern is always of stratified flow. In order to avoid the complication of the heat transfer correlation, equation (24) is applicable only to $G > 100$ kg/m^2 s.

Figs. 4 and 5 are respectively the comparisons of the prediction values of heat transfer coefficients with the experimental values of micro-fin tubes #1 and #2. It can be seen that there are about respectively 94% and 92% of the prediction values fall within ±30%. Table 6 is comparison of the error between the heat transfer coefficient prediction value and experimental value of micro-fin tube. For micro-fin tubes #1 and #2, equation (24) has respectively standard deviations of 25% and 20% on the heat transfer coefficient prediction.

5. Conclusion

This article mainly focuses on the evaporation heat transfer phenomenon of pure refrigerants in micro-fin tubes. The evaporation heat transfer characteristics of R-22 and R-124 were measured at the reduced pressure of 0.15, the mass flux from 100 to 400 kg/m^2 s, the flow quality from 0.1 to 0.9, and the heat flux from 5 to 20 kW/m^2 The experimental results show that the influences of heat flux on evaporation heat transfer coefficient in the micro-fin are obvious. The heat transfer coefficient increased with an increase of the heat flux. Since there are more nucleate cavity sites in the micro-fin tube, the evaporation heat transfer coefficient of refrigerant in micro-fin tube is larger than that of the smooth tube as compare to our past research [14]. This effect is more obvious at lower mass flux. The evaporation heat transfer coefficient of pure refrigerant in micro-fin tube is 1.5–3.0 times higher than that of smooth tube.

The single phase forced convection heat transfer coefficient of micro-fin tube is introduced to predict the evaporation heat transfer coefficient of pure refrigerant in micro-fin tubes. We can use equations (10)–(26) to predict the heat transfer coefficient of refrigerants; as compared to the experimental values, the predicted values mostly fall within ±30%. The present correlations provide reasonable agreement with the experimental data.

References

[1] S. Yoshida, T. Matsunaga, H.P. Hong, Heat transfer to refrigerants in horizontal evaporator tubes with internal spiral grooves, Proceedings of the ASME-JSME Thermal Engineering Joint Conference 5 (1987) 165–172.
[2] J.C. Khanpara, A.E. Bergle, M.B. Pate, Augmentation of R-113 in-tube evaporation with micro-fin tubes, ASHRAE Transactions 92 (2B) (1986) 506–524.
[3] L.M. Sohlagger, M.B. Pate, A.E. Bergles, Evaporation and condensation heat transfer and pressure drop in horizontal 12.7-mm micro-fin tubes with refrigerant 22, Journal of Heat Transfer 112 (1990) 1041–1045.
[4] S.J. Eckels, M.B. Pate, Evaporation and condensation of HFC-134a and CFC-12 in a smooth tube and a micro-fin tubes, ASHRAE Transactions 97 (2) (1991) 71–81.

[5] M.H. Kim, J.S. Shin, Evaporating heat transfer of R22 and R410A in horizontal smooth and microfin tubes, International Journal of Refrigeration 28 (2005) 940–948.
[6] R. Chiang, Heat transfer and pressure drop during evaporation and condensation of refrigerant-22 in 7.5 mm diameter axial and helical grooved tubes, AIChE Symposium Series 89 (295) (1993) 205–210.
[7] A. Greco, Convective boiling of pure and mixed refrigerants: an experimental study of the major parameters affecting heat transfer, International Journal of Heat and Mass Transfer 51 (2008) 896–909.
[8] J.R. Thome, Two-phase heat transfer to new refrigerants, 10Th International Heat Transfer Conference 1 (1994) 19–41.
[9] R.J. Moffat, Describing the uncertainties in experimental results, Experimental Thermal and Fluid Science 1 (1988) 3–17.
[10] Refprop NIST. National Institute of Standards and Technology, Gaithersburg, MD, 1994.
[11] R.K. Shah, Assessment of modified wilson plot techniques for obtaining heat exchanger design data, 9th International Heat Transfer Conference 5 (1990) 51–56.
[12] C.C. Wang, C.B. Chiou, D.C. Lu, Single-phase heat transfer and flow friction correlations for micro-fin tubes, International Journal of Heat and Fluid Flow 17 (5) (1996) 500–508.
[13] D. Steiner, J. Taborek, Flow boiling heat transfer in vertical tubes correlated by an asympototic model, Heat Transfer Engineering 13 (2) (1992) 43–69.
[14] C.B. Chiou, D.C. Lu, C.H. Chiou, A New correlation of forced convective boiling for pure and mixed refrigerants in horizontal smooth tube, Applied Thermal Engineering 29 (2009) 1864–1871.